Journal of Alloys and Compounds, 712 (2017) 373-378

Study of phases evolution in high-coercive MnAl powders obtained through short milling time of gas-atomized particles

J. Y. Law[1,3], J. Rial[1], M. Villanueva[1], N. López[1], J. Camarero[1], L. G. Marshall[2], J. S. Blázquez[3], J. M. Borrego[3], V. Franco[3], A. Conde[3], L. H. Lewis[2] and A. Bollero[1,a]

[1] *Division of Permanent Magnets and Applications, IMDEA Nanoscience, Campus Universidad Autónoma de Madrid, 28049 Madrid, Spain*

[2] *Department of Chemical Engineering, Northeastern University, Boston, MA 02115, USA*

[3] *Dpto. Física de la Materia Condensada, ICMSE-CSIC, Universidad de Sevilla, P.O. Box 1065, 41080 Sevilla, Spain*

Abstract

Gas-atomized $Mn_{54}Al_{46}$ particles constituted nominally of only ε- and γ_2-phases, i.e. no content of the ferromagnetic $L1_0$-type τ-phase, have been used to study the evolution of phases during short time of high-energy milling and subsequent annealing. Milling for 3 min is sufficient to begin formation of the τ-MnAl phase. A large coercivity of 4.9 kOe has been obtained in milled powder after annealing at 355 ºC for 10 minutes. The large increase in coercivity, by comparison with the lower value of 1.8 kOe obtained for the starting material after the same annealing conditions, is attributed to the combined formation of the τ-MnAl and β-Mn phases and the creation of a very fine microstructure with grain sizes on the order of 20 nm. Correlation between morphology, microstructure and magnetic properties of the rapidly milled MnAl powders constitutes a technological advance to prepare highly coercive MnAl powders.

Keywords: MnAl alloys; Ball milling; Permanent magnets; Nanostructured materials; Strain; Magnetic properties

[a] Corresponding author: alberto.bollero@imdea.org

1. Introduction

The increasing demand of permanent magnet-based technological applications as well as global scarcity issues of rare-earth (RE) resources are significant drivers that demonstrate the need for alternatives to conventional RE-based permanent magnets in many applications. Opening of new and previously closed mines has mitigated the supply risk of light REs (Nd, Pr) but this risk remains for heavy REs (Dy, Tb). Dysprosium (Dy) is needed to provide high coercive and maintain magnetic properties in NdFeB-based magnets. Independently of the lasting criticality of Dy, Nd remains a strategical material with a well-localized geographical distribution as production focuses relates. This situation has prompted a widespread search for RE-free permanent magnet alternatives. Among these alternatives, materials with economical raw material cost are identified as the established ferrites (oxides), Alnico magnets as well as Mn-based magnetic materials [1-3]. Mn-based permanent magnets have been regarded as promising to fill the performance gap between traditional ferrite and Alnico permanent magnets (energy product $(BH)_{max}$<10 MGOe) and the RE-based magnets ($(BH)_{max}$=20-30 MGOe) [1]. High magnetization and appreciable magnetic anisotropy are reported for binary Mn-based alloy systems, such as MnGa [4,5], MnBi [6,7] and MnAl [8,9], — with the abundant global distribution of Mn and Al resources in the earth's crust — have highlighted MnAl alloys as a promising choice among RE-free permanent magnets. This current work focuses on the coercivity development in MnAl powder obtained through milling and annealing by starting from $Mn_{54}Al_{46}$ alloy particles prepared by the gas-atomization technique.

The ferromagnetic τ-phase in the MnAl is metastable and forms from the non-magnetic and stable ε-phase. The mechanism of τ-phase transformation from the ε-phase is controversial. Some studies explain the origin of this transformation through a two steps process consisting first in the formation of an intermediary ε'-phase followed by a displacive shear mechanism

which transforms the ε'-phase to the τ-phase [10-12]. However, other studies refer to a "massive transformation" consisting of a compositionally invariant, difussional nucleation and growth process [13-15]. There are also reports combining both routes to explain the ε-to-τ phase transformation [16]. The structure and magnetic properties of the MnAl system have been widely studied because the microstructural changes and defects introduced during the metastable τ-phase transformation highly influence its magnetic properties. Studies have reported various techniques to prepare MnAl-based alloys, including hot extrusion, melt spinning, mechanical alloying, mechanical milling (MM), cryomilling, and gas-atomization [8,9,17-23]. Ball milling is a well-known technique used for microstructure refinement and strain inducement, but also for promotion of metastable phase formation. Previous studies show that high coercivities (above 4 kOe) can be achieved in MnAl after milling for a typical time duration of several to dozen of hours [20,21,24,25]. A coercivity of 5.3 kOe has been recently reported by Lu et al. [26] in isotropic MnAl powders by starting with melt-spun ribbons, annealing at 410 ºC for 30 min and subsequent milling for 23 hours. McCurrie et al. [27] obtained a maximum coercivity of 5 kOe for 63-75 μm particles obtained from grounding and sieving a slow cooled down MnAl ingot. Wei et al. [28] achieved the same maximum value of coercivity in MnAl melt-spun ribbons after annealing at 450ºC for 45 min followed by grinding for a shorter time of 90 min, at expenses of decreasing dramatically magnetization with increasing the grinding time. Zeng et al. [9] achieved a close maximum coercivity of 4.8 kOe in pre-alloyed powders after milling for 8 hours and annealing at 400 ºC. Additionally, it is noted that carbon additions to MnAl stabilizes the τ-phase. Recently, a short milling time of 1–1.5 hours applied to ternary MnAl-C alloys was reported to donate powder coercivities of H_c=4.1-4.6 kOe with τ-phase and ε-phase as starting materials, respectively [24].

In this current study, we use a rapid milling process that has been proven recently to be very efficient in tuning the microstructure for optimization of permanent magnet properties in

cobalt ferrite ($CoFe_2O_4$) [29]. Here we report a significant advance in binary MnAl alloys by achieving a coercivity of 4.9 kOe upon only 3 minutes of milling of MnAl gas-atomized particles followed by annealing at 355 ˚C for a short time (10 min). This annealing temperature is lower than the typical range of 400-700 ºC reported in the literature [18,26,28,30,31]. In contrast with previous studies, a side-by-side comparison is provided here of the evolution of morphological, microstructural and magnetic properties with annealing temperature of the powders in the as-atomized and as-milled forms, thereby allowing the effects of milling and of annealing to be identified.

2. Experimental

The starting material was gas-atomized powders of composition $Mn_{54}Al_{46}$ (±0.4 at.%). During the gas-atomization process, the molten alloy is atomized by inert gas jets into fine metal droplets which are quenched in the atomizing tower. Further details of these powders are published elsewhere [21]. Mechanical milling in a Planetary Fritz-Pulverisette for 3 minutes at rotation speed of 900 rpm was performed with tungsten carbide vials and balls with oleic acid as the surfactant. The powder-to-oleic acid ratio was 5:1, and the balls-to-powders mass ratio was 40:1. The loading and sealing of the vials were performed in an Ar-controlled atmosphere glove box. Both as-received and milled powders were annealed in N_2 with a ramp rate of 10 K/min at temperatures ($T_{annealing}$) of 350-475 ºC for 10 min. The samples were structurally and morphologically characterized using a Bruker D8 Advance A25 diffractometer with Cu Kα radiation and using a Zeiss-Evo scanning electron microscopy (SEM). Average crystallite sizes have been determined from application of the Scherrer formula to X-ray diffraction (XRD) patterns. Rietveld refinement of the XRD data was carried out to analyze the phase proportions and grain sizes of the starting and milled powders. The epsilon – tau structural transformations were studied using a Perkin–Elmer DSC-7 differential scanning calorimeter (DSC), with a temperature ramp rate of 20 K/min in

flowing argon gas. Upon cooling to room temperature, the samples were reheated in the DSC using the same experimental conditions to acquire a baseline for subsequent analysis. A high-purity sapphire sample in an Al pan was used as a standard for the DSC calibration. Magnetic properties were measured at room temperature using a Lakeshore 7400 series vibrating sample magnetometer with a maximum applied field of 20 kOe.

3. Results and discussion

3.1 Morphology and microstructure

XRD data and SEM images of the gas-atomized MnAl starting particles and particles milled for 3 minutes (prior to annealing) are presented in Fig. 1. The XRD pattern of the starting material [Fig. 1(a)] shows Bragg reflection peaks of ε- and γ_2-phases without any traces of τ-MnAl phase, within the limitations of the characterization technique, in agreement with the results of previous studies [20]. A milling time as short as 3 min is sufficient to initiate the transformation of the ε-phase into the τ-MnAl phase, as shown in Fig. 1(b), where coexistence of the three phases (τ, ε and γ_2) is found. The increased Bragg peak widths indicate reduced grain size and structural disorder induced by mechanical milling, which is typically reported for conventional milled MnAl systems (MM for 8-20 hours) [9,20,21]. Average crystallite sizes ~10 nm have been determined for both the remaining ε-phase and the newly formed τ-phase in the as-milled powders. This value contrasts with the mean crystallite size of about 100 nm determined for the ε-phase in the starting gas-atomized MnAl particles. Rietveld refinement of the XRD results reveals that 3 minutes of milling leads to the transformation of ε- to τ-phase (~20 weight % content). Microstructural modification induced by this short milling time becomes obvious from a direct comparison of the SEM images shown in Figs. 1(c) and 1(d), respectively. Approximately spherical particles with sizes of 10-40 μm are shown in Fig. 1(c) for the gas-atomized starting material. Milling for 3 minutes leads to a finer microstructure with flattened irregular-shaped morphologies with particle sizes ranging

from hundreds of nanometers to 10 μm in lateral size and a thickness varying from hundreds of nanometers to 1.5 μm.

DSC curves of starting and as-milled samples are shown in Figure 2. A prominent exothermic feature in the range 425 ºC < T < 500 ºC is observed for the starting gas-atomized sample, which corresponds to the ε→τ phase transformation. After a 3-min milling period, the DSC data indicates that the exothermic peak shifts to lower temperatures from a peak temperature of 472 ºC for the starting sample down to 395 ºC for the as-milled sample. In addition, an endothermic peak appears that is partially overlapped with the exothermic peak in the annealed sample, which is composed of various processes as indicated by the maxima found at 418 and 459 ºC. Such endothermic processes were previously observed at the initial steps of milling for Fe-based alloys, ascribed to the decomposition (pseudo-melting) of metastable intermetallics [32].

Figure 3 shows XRD patterns and Rietveld refinement results of the phase fractions existing after annealing at different temperatures (350-475 ºC for 10 min) for the starting gas-atomized particles [Figs. 3 (a) and (b), respectively] and for particles milled for 3 minutes [Figs. 3 (c) and (d), respectively].

Rietveld refinement indicates that the phase fraction of the starting powder is ~75 weight % ε-phase and ~25 weight % γ_2- phase. A decrease in the ε-phase fraction and an increase of τ- and β- phase content is observed with increasing the annealing temperature (T_{anneal}) [Fig. 3(b)]. The amount of γ_2-phase does not vary significantly with annealing temperature. Annealing of the as-atomized particles at T < 365 ºC [Fig. 3(a)] does not cause a significant change in the phase content of the powders, i.e., ε- and γ_2-phases [Fig. 1(a)]. However, annealing at T > 375 ºC yields an increase of the content of τ-phase at the expense of the ε-phase, and is accompanied by an increase of the amount of β-phase. The intensity of the diffraction peaks corresponding to τ-MnAl phase strongly increases with increasing T_{anneal}, as

shown in Fig. 3(a), signifying formation of additional τ-MnAl. The constitution of phases after annealing at the maximum temperature studied here (475ºC) is ~70 weight % τ-phase, 15 weight % β-phase and 15 weight % γ_2-phase, with no further detection by XRD of the ε-phase.

The distribution of phases is largely affected by the rapid milling procedure as a direct comparison of Figs. 3 (b) and (d) indicates. As shown in Figs. 1(b) and 3(d), milling for 3 min is sufficient to begin formation of τ-phase. The general trend for the phase constitution of as-milled particles [Fig. 3(d)] is a decrease of ε- and γ_2- fraction phases with increasing T_{anneal}, which is accompanied by an increase of the β-phase fraction content and a progressive decrease of the τ-phase content (after an initial increase for T_{anneal}<375 ºC). This behavior contrasts with the phase evolution previously observed for the as-atomized material [Fig. 3(b)], with a continuous increase of the τ-phase fraction in the complete temperature range under study. These results are in agreement with the observed DSC results, which showed a shift to lower temperatures of the nucleation of τ-phase and indicate that the transformation rate of τ-phase from its parent ε-phase is dependent on the ε-phase grain size [9,21]. The rapid milling process reduces the average crystallite size from 100 nm (starting as-atomized particles) to <10 nm, promoting the complete ε to τ transformation at T_{anneal}=365ºC, which is below the transformation temperature of 475ºC in non-milled material and below the typical transformation temperature range of 400-700 ºC reported in the literature [18,30,31]. The diffraction peaks of the β-phase shift to lower angles in comparison to a pure β-Mn phase, and the measured lattice parameter of the cubic β-phase (a=0.6444±0.003 nm) is closer to that of β-Mn_3Al_2 (a=0.63245 nm, $P4_132$), which has been also reported for 10 h-milled MnAl-based systems [33,34]. This result might be an indication that milling followed by annealing allows the metastable τ-MnAl phase to transform into β-Mn(Al) phase, with a composition close to Mn_3Al_2. No β-Mn(Al) phase was observed prior to annealing in as-milled powders. Annealing at 375 ºC for a short time of 10 minutes guarantees the total disappearance of the ε-phase

present in the as-milled powder and results in ~30 wt% of τ-, ~50 wt% of β- and ~20 wt% of γ_2- phase fractions [Fig. 3(c)]. The rather low content of τ-MnAl phase is mainly due to the absence of 100 weight % content of ε-phase in the starting gas-atomized MnAl particles (but 75 weight %).

3.2 Magnetic properties

Representative hysteresis curves of starting and as-milled powders prior to and after annealing are presented in Fig. 4. The starting gas-atomized MnAl powders (inset Fig. 4) are paramagnetic consistent with absence of ferromagnetic τ-MnAl in the XRD data (Fig. 3) and in accordance with previous results [20]. Ferromagnetism is detected after rapid milling of only 3 minutes without any post-annealing treatment, indicating the presence of the τ-MnAl phase, and consistent with the XRD results [Figs. 1 and 3(b)]. This direct transformation of ε- to τ-MnAl phase through milling with no need of annealing has been recently reported in cryomilled MnAl ribbons [12]. Mechanical milling at cryogenic temperatures suppresses the high temperatures (typically hundreds of degrees) locally achieved during conventional milling, demonstrating the possibility of direct ε- to τ-MnAl phase transformation in the process [12]. By contrast with that study, the starting material here used does not contain the τ-MnAl phase, but it is only formed after milling. The use of a very short milling time likely avoids large temperature excursions achieved when milling for long times (typically several hours). The refinement of the ε-phase through milling and the likely microstrain induced during the process are concluded to be beneficial factors determining the ε- to τ- phase transformation during the milling process [Fig. 3(d)] [12,26]. These results are consistent with a strain induced ε-to-τ phase transformation in good agreement with the result obtained by Marshall et al. [12] by using cryomilling and, in a similar manner, with no need of annealing to ease the transformation.

Annealing affects very differently the shape of the hysteresis loops of the as-prepared and the as-milled powders, demonstrating the strong effect that the rapid milling procedure has on the

morphology and microstructure of the gas- atomized MnAl particles (Fig. 4). Annealing of the milled powders at 355 ºC results in improved magnetic properties (H_c=4.9 kOe; M_r=12.9 emu/g; M_s=22.6 emu/g) relative to those measured for the gas-atomized particles after identical heat treatment (H_c=1.8 kOe; M_r=0.3 emu/g; M_s=1.9 emu/g). This improvement is directly related to two factors: first, the beginning of crystallization of τ-MnAl phase in the as-milled powders, and second, to the enhanced ε- to τ- phase transformation produced by annealing the highly refined ε-phase (~ 5 nm grain size). Annealing at a higher temperature of 375 ºC improves further the magnetic properties (Fig. 4) for both materials. This result is attributed to an increased τ-MnAl phase content (~10 and ~30 wt%, respectively) as well as to microstructural changes introduced by the milling process, which directly influence coercivity. This latter aspect will be discussed in the following section.

Figure 5(a) shows the evolution of coercivity with annealing temperature for the as-atomized material and the as-milled powder. The first observation is the attainment of a coercivity that is approximately three times larger than those found in milled and annealed powders over the complete annealing temperature range of this study. This result indicates the effectiveness of the rapid (3 min) milling procedure to increase H_c of gas-atomized MnAl particles followed by annealing for a short time. In specific, annealing the as-milled powder at 350 ºC for 10 min results in a large value of coercivity, H_c=4.5 kOe. The largest coercivity of 4.9 kOe is obtained for the milled powders after annealing at 355 ºC, while the as-atomized material shows maximum H_c=2.0 kOe after annealing at 365 ºC. Relatively low remanence and magnetization measured at 20 kOe maximum field, M_{20kOe}, values of 7.7 and 16.4 emu/g [Fig. 5(b)], respectively, are attributed to the rather low content (about ~25 wt%) of τ-MnAl phase [Fig. 3(d)] in this stage of the processing. However, a maximum applied field of 20 kOe is not sufficient to fully saturate the samples under study, as shown in the hysteresis loops from Fig. 4. The main factors that contribute to the much larger coercivity obtained for the as-milled MnAl powders are the increased content of the hard ferromagnetic phase τ-MnAl and

formation of the β-Mn phase, and the reduced grain size of the τ-MnAl phase resulting in an enlarged number of grain boundaries. The average crystallite size increased from ~20 nm (T_{anneal}=350 ºC) to ~80 nm (T_{anneal}>350 ºC) for the milled samples annealed with yet higher values after annealing at the maximum studied temperature of 475 ºC. Annealing at 400 ºC results in about ~50 and ~30 wt% content of τ-MnAl phase for the as-atomized and for the milled particles, respectively, i.e. a significantly larger fraction of τ-MnAl phase present in the former. However, the coercivity of the annealed as-atomized particles remains much lower (1.5 kOe) than that of the milled and annealed counterparts (4.6 kOe). Consequently, it is concluded that the formation of milling-induced defects may act as strong domain wall pinning centers in this system [8,12,30,31,35,36]. Based on the different phase fractions found in materials subjected to different annealing temperatures, [Figs. 3 (b) and (d)], it is hypothesized that the non-magnetic β-Mn(Al) phase plays a determinant role pinning domain walls, as suggested in previous studies [8,9,23,37-40].

Magnetic remanence follows the same trend with annealing temperature as the M_{20kOe} for both starting and as-milled particles [Fig. 5(b)]. The stepped increased of M_{20kOe} and M_r with increasing T_{anneal} measured for the starting material in the complete temperature range under study (350-475 ºC), is a consequence of the enhanced content in the ferromagnetic τ-MnAl phase with annealing temperature shown in Fig. 3(b). However, for the as-milled powders, the evolution of magnetization with T_{anneal} does not follow the same evolution of τ-MnAl phase content. The magnetization values M_{20kOe} and M_r increase in the temperature range 350-375ºC while, by looking at the evolutions of the phase fractions in Fig. 3(d), the τ-MnAl phase content remains approximately constant in the range 350-375 ºC. This increase in magnetization could be attributed to an enhanced order of the τ-MnAl phase in the as-milled powders achieved through annealing [23,41,42].

It is hypothesized that the highly energetic rapid milling procedure promotes the formation of τ-MnAl phase through a combination of local heating and the creation of dislocations in the

starting material to promote the ε- to τ-MnAl phase transformation. However, the level of ordering of the created τ-MnAl phase has been shown to be also of importance to explain the evolution of the magnetization [9,12,20,21]. Disorder induced during milling might result in Mn atoms occupying Al sites and, consequently, decreasing the ferromagnetism due to the antiferromagnetic coupling between Mn atoms on A and B sites in the lattice, i.e. reducing the magnetization. In fact, the superlattice (100) diffraction maximum of the τ-phase is absent for as-milled powder but is detected after annealing. Subsequent annealing further promotes the ordering process and therefore increases magnetization. However, annealing above 375ºC leads to the decomposition of the τ-MnAl phase into the β-phase [Fig. 3(d)] resulting in the observed decrease in magnetization [Fig. 5(b)].

Conclusions

Gas-atomized MnAl particles constituted nominally by ε- and γ_2-phases have been milled for a short time of 3 min in Ar using oleic acid as a surfactant. This rapid milling procedure results in the formation of the ferromagnetic τ-MnAl phase from transformation of the initial paramagnetic ε-phase. A large coercivity of 4.9 kOe has been attained after annealing the 3-minutes milled powder at 355 ºC for 10 minutes. This coercivity value demonstrates a 2.5-fold enhancement compared to the largest coercivity of its unmilled counterparts (2.0 kOe). Magnetization remains however rather low due to the reduced content (below 30 wt.%) of the τ-MnAl phase obtained after milling and annealing. The large coercivity achieved in milled and annealed powders is demonstrated to result from refinement of the microstructure and to the combined effect of the transformation of ε- to τ-MnAl phase and the formation of the non-magnetic β-phase. Formation of the β-phase is promoted with increased annealing temperature and it is concluded that the β-phase plays a role in enhancing the coercivity, most likely through a domain wall pinning mechanism. This study demonstrates the possibility of

achieving highly coercive isotropic MnAl powders - among the largest coercivities reported- for binary MnAl alloys- with an extremely short milling processing time.

Acknowledgements

The gas-atomized powders were provided by Prof. Ian Baker, Dartmouth College where they were produced via a grant from the U.S. Department of Energy, Advanced Research Projects Agency – Energy (ARPA-E) through REACT program contract no. DE-AR0000188. This research has been funded by MINECO (Spanish Ministry of Science and Innovation): ENMA-National project (MAT2014-56955-R) and Northeastern University, MINECO through M-era.Net Programme: NEXMAG project (PCIN-2015-126) and Regional Government (Comunidad de Madrid): NANOFRONTMAG (Ref. S2013/MIT-2850), MINECO (project MAT2013-45165-P) and the PAI of the Regional Government of Andalucía.

References

[1] I. Baker, Manganese-based Permanent Magnets, Metals 5 (2015) 1435.
[2] K. Anand, J. J. Pulikkotil, and S. Auluck, Study of ferromagnetic instability in τ-MnAl, using first-principles, Journal of Alloys and Compounds 601 (2014) 234-237.
[3] J. M. Coey, Hard Magnetic Materials: A Perspective, IEEE Transactions on Magnetism 47 (2011) 4671-4681.
[4] T. J. Nummy, S. P. Bennett, T. Cardinal, and D. Heiman, Large coercivity in nanostructured rare-earth-free MnxGa films, Applied Physics Letters 99 (2011) 252506 .
[5] S. Mizukami, F. Wu, A. Sakuma, J. Walowski, D. Watanabe, T. Kubota, X. Zhang, H. Naganuma, M. Oogane, Y. Ando, and T. Miyazaki, Long-Lived Ultrafast Spin Precession in Manganese Alloys Films with a Large Perpendicular Magnetic Anisotropy, Physical Review Letters 106 (2011) 117201.
[6] C. Chinnasamy, M. M. Jasinski, A. Ulmer, L. Wanfeng, G. Hadjipanayis, and J. Liu, Mn-Bi Magnetic Powders With High Coercivity and Magnetization at Room Temperature, IEEE Transactions on Magnetism 48 (2012) 3641.
[7] J. B. Yang, K. Kamaraju, W. B. Yelon, W. J. James, Q. Cai, and A. Bollero, Magnetic properties of the MnBi intermetallic compound, Applied Physics Letters 79 (2001) 1846.
[8] Q. Zeng, I. Baker, and Z.-C. Yan, Nanostructured Mn–Al permanent magnets produced by mechanical milling, Journal of Applied Physics 99 (2006) 08E902.
[9] Q. Zeng, I. Baker, J. B. Cui, and Z. C. Yan, Structural and magnetic properties of nanostructured Mn–Al–C magnetic materials, Journal of Magnetism and Magnetic Materials 308 (2007) 214-226.

[10] J. Van Den Broek, H. Donkersloot, G. Van Tendeloo, and J. Van Landuyt, Phase transformations in pure and carbon-doped $Al_{45}Mn_{55}$ alloys, Acta Metallurgica 27 (1979) 1497.

[11] V. Rao, S. Pramanik, C. R. Tewari, S. R. Singh, and O. N. Mohanty, Phase transformations in Mn-Al permanent magnet alloys, Journal of Materials Science 24 (1989) 4088.

[12] L. G. Marshall, I. J. McDonald, and L. H. Lewis, Quantification of the strain-induced promotion of τ-MnAl via cryogenic milling, Journal of Magnetism and Magnetic Materials 404 (2016) 215.

[13] D. P. Hoydick, E. J. Palmiere, and W. A. Soffa, Microstructural development in MnAl-base permanent magnet materials: New perspectives, Journal of Applied Physics 81 (1997) 5624.

[14] C. Yanar, J. M. K. Wiezorek, V. Radmilovic, and W. A. Soffa, Massive transformation and the formation of the ferromagnetic $L1_0$ phase in Manganese-Aluminum-based alloys, Metallurgical and Materials Transactions A 33 (2002) 2413.

[15] I. Janotová, P. _Svec Sr., P. _Svec, I. Mat'ko , D. Janickovic, J. Zigo , M. Mihalkovic, J. Marcin, and I. Skorvánek, Phase analysis and structure of rapidly quenched Al-Mn systems, Journal of Alloys and Compounds (2016) http://dx.doi.org/10.1016/j.jallcom.2016.11.171

[16] J. M. K. Wiezorek, A. K. Kulovits, C. Yanar, and W. A. Soffa, Grain Boundary Mediated Displacive–Diffusional Formation of τ-Phase MnAl, Metallurgical and Materials Transactions A 42 (2011) 594.

[17] Z. W. Liu, C. Chen, Z. G. Zheng, B. H. Tan, and R. V. Ramanujan, Phase transitions and hard magnetic properties for rapidly solidified MnAl alloys doped with C, B, and rare earth elements, Journal of Materials Science 47 (2011) 2333-2338.

[18] T. Saito, Magnetic properties of Mn–Al system alloys produced by mechanical alloying, Journal of Applied Physics 93 (2003) 8686.

[19] Z. C. Yan, Y. Huang, Y. Zhang, G. C. Hadjipanayis, W. Soffa, and D. Weller, Magnetic and structural properties of MnAl/Ag granular thin films with L10 structure, Scripta Materialia 53 (2005) 463.

[20] A. Chaturvedi, R. Yaqub, and I. Baker, A comparison of τ-MnAl particulates produced via different routes, J Phys Condens Matter 26 (2014) 064201.

[21] A. Chaturvedi, R. Yaqub, and I. Baker, Microstructure and Magnetic Properties of Bulk Nanocrystalline MnAl,Metals 4 (2014) 20.

[22] F. Jiménez-Villacorta, J. Marion, J. Oldham, M. Daniil, M. Willard, and L. Lewis, Magnetism-Structure Correlations during the ε→τ Transformation in Rapidly-Solidified MnAl Nanostructured Alloys, Metals 4 (2014) 8.

~~[16] L. G. Marshall, I. J. McDonald, and L. H. Lewis, Quantification of the strain-induced promotion of τ-MnAl via cryogenic milling, Journal of Magnetism and Magnetic Materials 404 (2016) 215-220.~~ Listed now as Ref. 12

[23] X. Wang, J. Lee, J. Lee, H. Kim, C. Choi, and Z. Zhang, Structural and magnetic properties of the gas atomized Mn-Al alloy powders, Metals and Materials International 18 (2012) 711-715.

[24] M. Lucis, T. Prost, X. Jiang, M. Wang, and J. Shield, Phase Transitions in Mechanically Milled Mn-Al-C Permanent Magnets, Metals 4 (2014) 130-140.

[25] A. M. Gabay and G. C. Hadjipanayis, Application of Mechanochemical Synthesis to Manufacturing of Permanent Magnets, JOM 67 (2015) 1329-1335.

[26] W. Lu, J. Niu, T. Wang, K. Xia, Z. Xiang, Y. Song. H. Zhang, S. Yoshimura, and H. Saito, Low-energy mechanically milled τ-phase MnAl alloys with high coercivity and magnetization, Journal of Alloys and Compounds 675 (2016) 163-167.

[27] R. A. McCurrie, J. Rickman, P. Dunk, and D. G. Hawkridge, "Dependence of the permanent magnet properties of Mn55Al45 on particle size", IEEE Transaction on Magnetics 14 (1978) 682.

[28] J. Z. Wei, Z. G. Song, Y. B. Yang, S. Q. Liu, H. L. Du, J. Z. Han, D. Zhou, C. S. Wang, Y. C. Yang, A. Franz, D. Többens, and J. B. Yang, "τ-MnAl with high coercivity and saturation magnetization", AIP Advances 4 (2014) 127113.

[29] F. J. Pedrosa, J. Rial, K. M. Golasinski, M. Rodríguez-Osorio, G. Salas, D. Granados, J. Camarero, and A. Bollero, Tunable nanocrystalline CoFe2O4 isotropic powders obtained by co-precipitation and ultrafast ball milling for permanent magnet applications, RSC Adv. 6 (2016) 87282-87287.

[30] H. Jian, K. P. Skokov, and O. Gutfleisch, Microstructure and magnetic properties of Mn–Al–C alloy powders prepared by ball milling, Journal of Alloys and Compounds 622 (2015) 524-528.

[31] J. P. Jakubovics and T. W. Jolly, The effect of crystal defects on the domain structure of Mn-Al alloys, Physica 86-88B (1977) 1357-1359.

[32] J. S. Blázquez, J. J. Ipus, M.Millán, V. Franco, A. Conde, D. Oleszak, T. Kulik, Supersaturated solid solution obtained by mechanical alloying of 75% Fe, 20% Ge and 5% Nb mixture at different milling intensities, Journal of Alloys and Compounds 469 (2009) 169-178.

[33] J. M. Le Breton, J. Bran, E. Folcke, M. Lucis, R. Lardé, M. Jean, and J. E. Shield, Structural modifications in a Mn54Al43C3 melt-spun alloy induced by mechanical milling and subsequent annealing investigated by atom probe tomography, Journal of Alloys and Compounds 581 (2013) 86-90.

[34] S. Mican, D. Benea, R. Hirian, R. Gavrea, O. Isnard, V. Pop, and M. Coldea, Structural, electronic and magnetic properties of the Mn50Al46Ni4 alloy, Journal of Magnetism and Magnetic Materials 401 (2016) 841-846.

[35] R. Skomski, Nanomagnetics, J. Phys.: Condens. Matter 15 (2003) R841-R896.

[36] S. H. Nie, L. J. Zhu, J. Lu, D. Pan, H. L. Wang, X. Z. Yu, J. X. Xiao, and J. H. Zhao, Perpendicularly magnetized τ-MnAl (001) thin films epitaxied on GaAs, Applied Physics Letters 102 (2013) 152405.

[37] M. A. Bohlmann, J. C. Koo, and J. H. Wise, Mn-Al-C for permanent magnets, J. Appl. Phys. 52 (1981) 2542.

[38] J. D. Livingston, A review of coercivity mechanisms, J. Appl. Phys. 52 (1981) 2544.

[39] J. H. Huang and P. C. Kuo, Sintered MnAl and MnAlC magnets, Mater. Sci. Eng. B 14 (1992) 75-79.

[40] T. D. Shen, R. B. Schwarz, and J. D. Thompson, Soft magnetism in mechanically alloyed nanocrystalline materials, Phys. Rev. B 72 (2005) 014431.

[41] A. J. J. Koch, P. Hokkeling, M. G. V. D. Sterg, and K. J. DeVos, New material for permanent magnets on a base of Mn and Al, J. Appl. Phys. 31 (1960) 75S.

[42] W. Van Roy, H. Bender, C. Bruynseraede, J. De Boeck, and G. Borghs, Degree of order and magnetic properties of τ-MnAl films, J. Magn. Magn. Mater. 148 (1995) 97-98.

Figure Captions

Figure 1. (Color on-line). XRD data of (a) starting gas-atomized MnAl particles and (b) powder after milling for 3 minutes. SEM images of (c) starting and (d) 3 min milled gas-atomized MnAl (scale bar: 50 μm).

Figure 2. (Color on-line). DSC curves of starting (continuous line) and as-milled (dashed line) samples, measured at a heating rate of 20 K/min.

Figure 3. (Color on-line). XRD data of (a) starting gas-atomized MnAl material and (b) milled upon annealing. Rietveld refinement results of the existing phase fractions in (c) starting material and (d) milled samples, obtained from XRD results (a) and (b), respectively.

Figure 4. (Color on-line). Hysteresis loops of starting (gas-atomized MnAl particles) and as-milled samples annealed at selected temperatures. Inset: Hysteresis loops for starting material [square symbols] and milled (3 min) powders [circles].

Figure 5. (Color on-line). Influence of annealing temperature on (a) coercivity, H_c, and (b) remanence, M_r, and magnetization measured with a maximum applied field of 20 kOe, M_{20kOe}, for non-milled and milled gas-atomized MnAl samples.

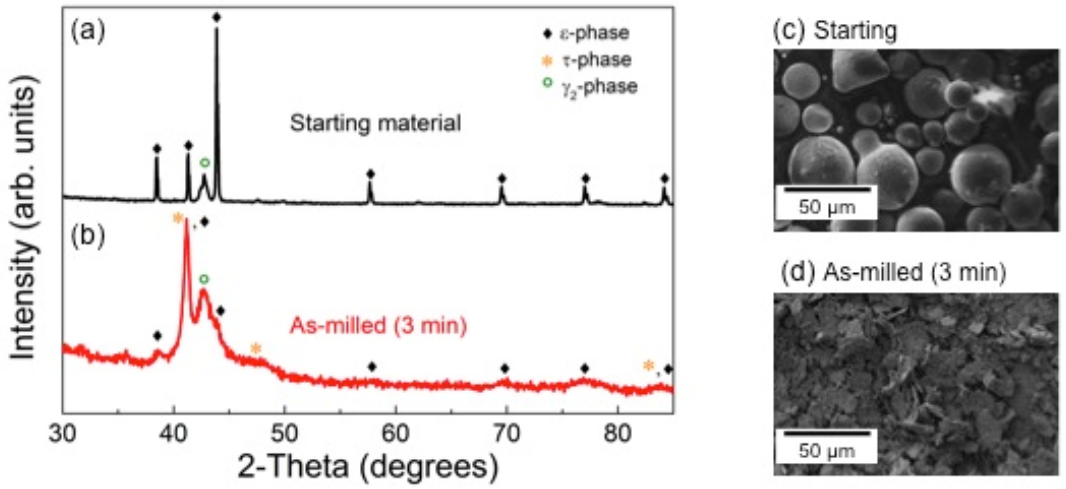
(a)
ε-phase
τ-phase
γ2-phase
Starting material
(b)
As-milled (3 min)
Intensity (arb. units)
30
40
50
60
70
80
2-Theta (degrees)
(c) Starting
50 μm
(d) As-milled (3 min)
50 μm

Figure 1

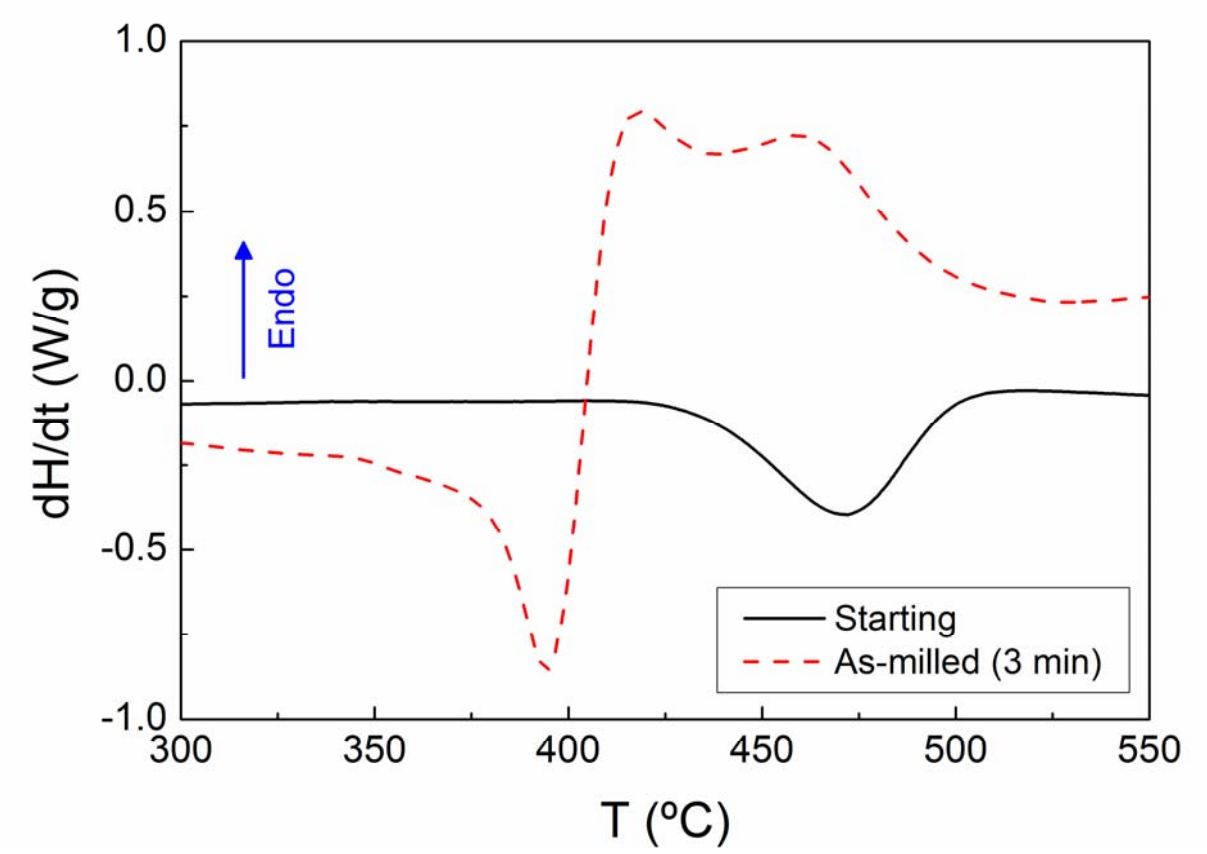
1.0
0.5
0.0
-0.5
-1.0
dH/dt (W/g)
Endo
300
350
400
450
500
550
T (ºC)
Starting
As-milled (3 min)

Figure 2

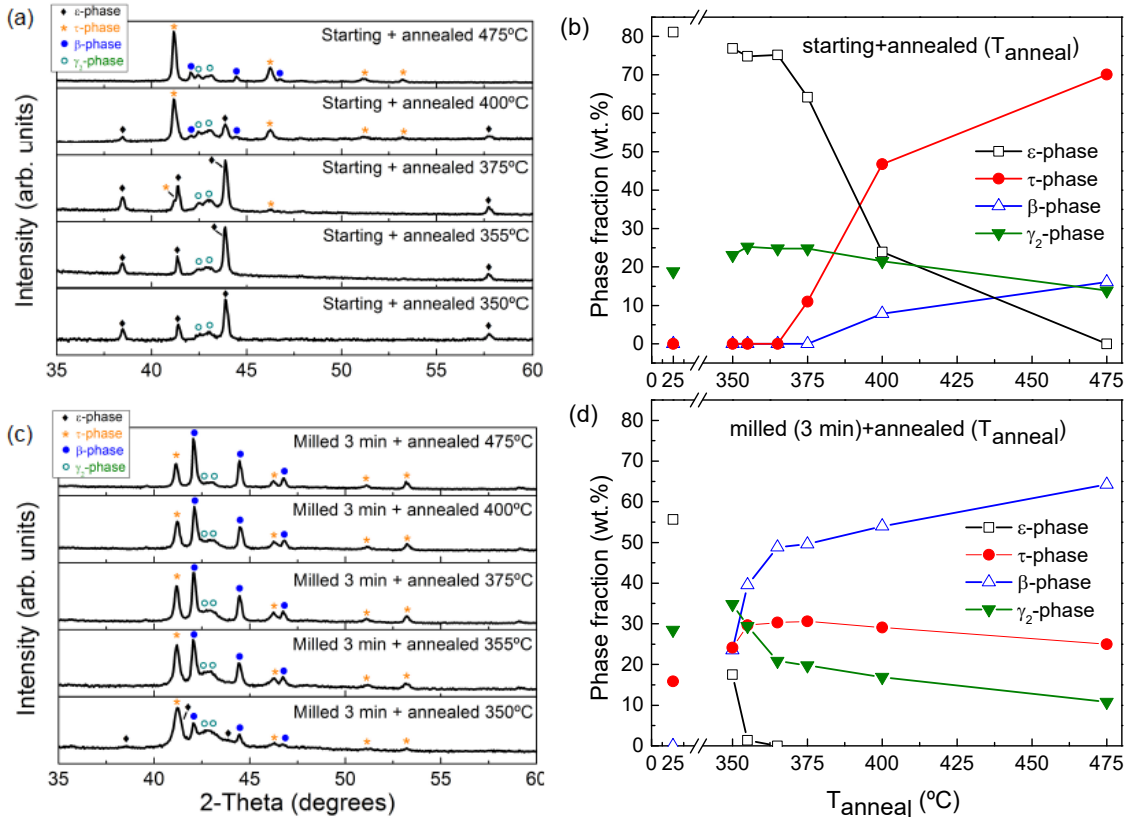
(a)
ε-phase
τ-phase
β-phase
γ2-phase
Starting + annealed 475ºC
Starting + annealed 400ºC
Starting + annealed 375ºC
Starting + annealed 355ºC
Starting + annealed 350ºC
Intensity (arb. units)
35 40 45 50 55 60
(b)
starting+annealed (Tanneal)
Phase fraction (wt.%)
0 10 20 30 40 50 60 70 80
0 25 350 375 400 425 450 475
ε-phase
τ-phase
β-phase
γ2-phase
(c)
Milled 3 min + annealed 475ºC
Milled 3 min + annealed 400ºC
Milled 3 min + annealed 375ºC
Milled 3 min + annealed 355ºC
Milled 3 min + annealed 350ºC
Intensity (arb. units)
35 40 45 50 55 60
2-Theta (degrees)
(d)
milled (3 min)+annealed (Tanneal)
Phase fraction (wt.%)
0 10 20 30 40 50 60 70 80
0 25 350 375 400 425 450 475
Tanneal (ºC)
ε-phase
τ-phase
β-phase
γ2-phase

Figure 3

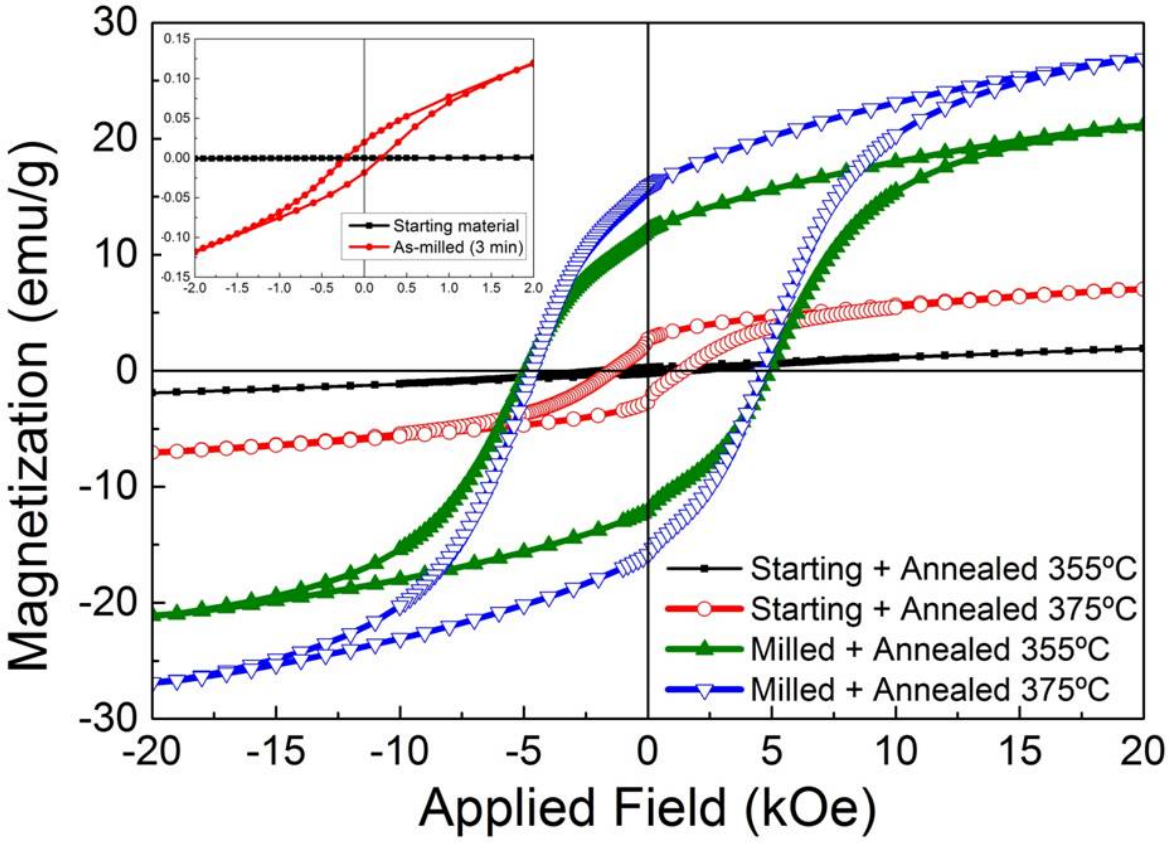
Magnetization (emu/g)
Applied Field (kOe)
Starting + Annealed 355ºC
Starting + Annealed 375ºC
Milled + Annealed 355ºC
Milled + Annealed 375ºC
Starting material
As-milled (3 min)

Figure 4

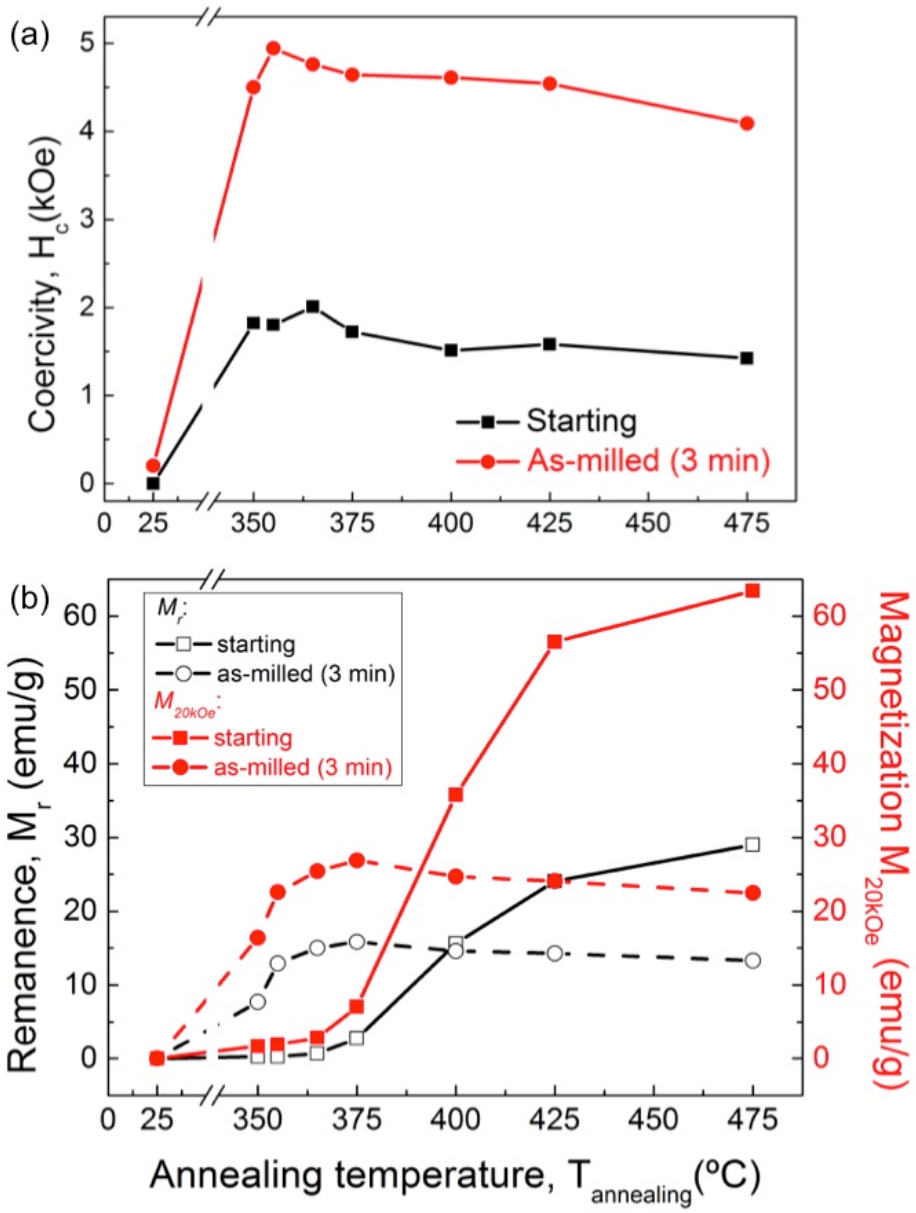
(a)
Coercivity, H_c(kOe)
Starting
As-milled (3 min)
(b)
M_r:
starting
as-milled (3 min)
M_{20kOe}:
starting
as-milled (3 min)
Remanence, M_r (emu/g)
Magnetization M_{20kOe} (emu/g)
Annealing temperature, $T_{annealing}$(°C)

Figure 5